Segmentation Under Occlusions Using Selective Shape Prior*

Sheshadri R. Thiruvenkadam[1], Tony F. Chan[1], and Byung-Woo Hong[2]

[1] Department of Mathematics
[2] Computer Science Department
University of California, Los Angeles, CA-90095, USA
sheshad,chan@math.ucla.edu, hong@cs.ucla.edu

Abstract. In this work, we address the problem of segmenting multiple objects, with possible occlusions, in a variational setting. Most segmentation algorithms based on low-level features often fail under uncertainties such as occlusions and subtle boundaries. We introduce a segmentation algorithm incorporating high-level prior knowledge which is the shape of objects of interest. A novelty in our approach is that prior shape is introduced in a selective manner, only to occluded boundaries. Further, a direct application of our framework is that it solves the *segmentation with depth* problem that aims to recover the spatial order of overlapping objects for certain classes of images. We also present segmentation results on synthetic and real images.

1 Introduction

Image segmentation is an important step in understanding the composition of the original 3D scene that gave rise to the image. However, it is often considered as a difficult problem due to noise which results in spurious edges and boundary gaps, and occlusions which leads to a overlap of object boundaries. Low-level visual features such as intensity, color and texture are generally not sufficient to overcome such difficulties that would make purely bottom-up segmentation approaches unsuccessful. This naturally leads to a need for integrating low-level features and high-level information in segmentation. Enforcing a prior knowledge on the shape of objects is a common way to facilitate segmentation specially under low contrasts, occlusions and other undesirable noisy conditions.

In this paper, we address the problem of segmenting multiple objects with possible occlusions. Here, a segmentation method incorporating shape prior knowledge is presented in a variational approach using the level set framework [15]. The level set framework is commonly used in segmentation [10,1,8,16,3,17] due to the following favorable properties: it provides an implicit boundary representation that is free of parameterization, easily deals with topological changes of the boundary such as splitting and merging, and can be naturally extended to any dimension.

* Supported by ONR grant N00014-06-1-0345 and NSF grant DMS-0610079.

F. Sgallari, A. Murli, and N. Paragios (Eds.): SSVM 2007, LNCS 4485, pp. 191–202, 2007.

A level set implementation of active contours with region-based image terms using the Mumford-Shah functional [12] has been developed by Chan and Vese [3]. This is shown to be robust with respect to noise due to the intrinsic smoothness terms that regularize the shape of the segmenting contours and also allows the segmentation of multiple objects [18]. However, this method solely relies on image intensity which is not sufficient to overcome occlusions that occur in many practical applications. This consequently leads to the efforts that introduce prior shape information into segmentation schemes based on level sets. The active shape model [5] using principal component analysis from a set of training shapes has been used as prior shape information and incorporated with level set implementation in [17,9,11], where a statistical shape model is employed. In [4,2], the authors have proposed a variational method where the energy function that governs the evolution of the level set function depends on image information and shape information. In contrast to a conventional linear PCA, a nonlinear statistics by means of kernel PCA is considered as a shape model in [6].

Although incorporating a shape prior within our segmentation model was inspired by the above works, our method has a novelty in that, the use of shape prior knowledge is automatically restricted *only* to occluded parts of the object boundaries. This selective use of local prior shape avoids enforcing prior shape on regions where the object boundary is clearly characterized by image intensity.

A direct application of our approach is that it solves the *segmentation with depth* problem that aims to determine the boundaries of the overlapping objects, along with their spatial ordering, based on the intensity distributions in the object regions. The segmentation with depth problem has been addressed before in a variational framework by Nitzberg, Mumford and Shiota (NMS) in [13,14] and numerical methods for minimizing the NMS model have been presented in [7]. The NMS model is closely related to our segmentation model and their differences will be discussed later.

2 Occlusion Model

Suppose that $I : \Omega \to \mathbb{R}$, $\Omega \subset \mathbb{R}^2$ is a 2D image of a scene composed of N objects $\{O_p\}_{p=1}^N$. Let $\{A_p\}_{p=1}^N$ be the regions formed on the image domain by the objects. Now suppose that we have the following assumptions:

- The image intensity formed by the object O_k is close to a constant c_k, and the background intensity is close to a constant, $\tilde{c}$.
- The objects are not twisted between themselves.

One way to represent such an occlusion scene is as a linear combination of the background, the object regions, and their intersection regions (where occlusions possibly occur). To motivate the form of I, we see in the case $N = 3$, suppose that $O_1,\ O_3,\ O_2$ is the spatial order of the objects,

$$I = c_1\chi_{A_1} + c_2\chi_{A_2} + c_3\chi_{A_3} - c_2\chi_{A_1\cap A_2} - c_2\chi_{A_2\cap A_3} - c_3\chi_{A_1\cap A_3}$$
$$+c_2\chi_{A_1\cap A_2\cap A_3} + \tilde{c}(1-\chi_{A_1})(1-\chi_{A_2})(1-\chi_{A_3})$$

where χ_S is the characteristic function of a set S.

In general, for N objects, the image I is of the form,

$$I = \sum_{p=1}^{N} \sum_{k=1}^{\binom{N}{p}} (-1)^{p-1} c_{p,k} \chi_{P_{p,k}} + \tilde{c} \prod_{k=1}^{N} (1 - \chi_{A_k}) \tag{1}$$

Here, $P_{p,k}$, $(p = 1, 2..N, k = 1, 2, ..\binom{N}{p})$ is the k^{th} unordered intersection of p regions from $A_1, A_2, ..., A_N$. $c_{p,k}$ are positive constants, with $c_{1,k} = c_k$, and for $p > 1$, $c_{p,k}$ takes one of the values $c_1, c_2, ...c_N$, depending entirely on the occlusion relationships between the objects.

In fact, there are $N!$ different possible sequences for $c_{p,k}$, $p > 1$, with each sequence corresponding to a particular spatial ordering of the objects. For instance, for the $N = 2$ case, $I = c_1\chi_{A_1} + c_2\chi_{A_2} - c_{2,1}\chi_{A_1 \cap A_2} + \tilde{c}(1-\chi_{A_1})(1-\chi_{A_2})$, and we see that, $c_{2,1} = c_2(c_1)$ iff $A_1(A_2)$ occludes $A_2(A_1)$.

In this work, given an image I_0, we solve the inverse problem of recovering the object regions $\{A_p\}_{p=1}^{N}$, and constants $c_{p,k}$, $p = 1, 2..N, k = 1, 2, ..\binom{N}{p}$. We formulate the above problem as the following energy minimization. Here, we have also added a term within the energy that captures shape of the objects (to resolve occluded boundaries).

$$E := \int_{\Omega} (I_0 - (\sum_{p=1}^{N} \sum_{k=1}^{\binom{N}{p}} (-1)^{p-1} c_{p,k} \chi_{P_{p,k}} + \tilde{c} \prod_{k=1}^{N} (1 - \chi_{A_k})))^2 dx + \sum_{p=1}^{N} (\lambda \int_{\partial A_p} ds + \beta \int_{\Omega} \hat{S}(A_p) dx) \tag{2}$$

The second term is a length regularization term, and the third term constrains the shape of the boundaries of A_k. Note that in the forward model (1), the constants $c_{p,k}$ satisfy at least one of $N!$ constraints corresponding to $N!$ possible spatial ordering for the objects. Here, for computational simplicity, we have assumed the constants $c_{p,k}$ to be independent, and minimize (2) without constraints. Then, we show in section 5. that for images satisfying certain conditions, the recovered constants $c_{p,k}$ can be used to solve occlusion relationships between the objects (hence solving the segmentation from depth problem). Later, in section 6, we show how these relationships can be used to selectively impose shape constraints, only to occluded object boundaries.

3 Related Works

As mentioned in the previous section, the inverse problem we are looking at is related to the segmentation with depth problem. Here, we will briefly review the related formulation of NMS [14] for segmentation with depth and present comparisons with our approach.

Using the same terminology used as before, let $A_1, A_2, ..., A_N$ be the regions on the image plane corresponding to the objects $O_1, O_2, .., O_N$, with corresponding

constant intensity $c_1, c_2, ..c_N$. Also assume that the objects are spatially ordered, i.e, if $i < j$ then O_i is on top of O_j. Then, the non-occluded (visible) part of O_i, $\tilde{A}_i$ is $\tilde{A}_i = A_i - \bigcup_{j<i} A_j$, for $i > 1$. Let $\tilde{A}_1 = A_1$. Then the image formed by this ordering of O_k is:

$$I = \sum_{i=1}^{N} c_i \chi_{\tilde{A}_i} \tag{3}$$

To start with, we note that our occlusion model (1) and (3) can be shown to be equivalent. For instance, in the two object case, we verify that if A_1 occludes A_2, then (3) gives $I = c_1\chi_{A_1} + c_2\chi_{A_2 - A_1}$ which can be rewritten as $I = c_1\chi_{A_1} + c_2\chi_{A_2} - c_2\chi_{A_1 \cap A_2}$, which is our model shown in (1).

In (NMS), the authors look at the inverse problem of solving for A_k, c_k, and the ordering of the objects O_k, from a given image I_0, by considering the following minimization:

$$\tilde{E} := \sum_{i=1}^{N} \int_{\tilde{A}_i} (I_0 - c_i)^2 dx + \int_{\partial A_i} (\alpha + \beta\phi(k)) ds \tag{4}$$

where the function $\phi(x)$ is to be a positive, convex, even function. The above energy is minimized for each possible order relation between O_k (a total of $N!$ energy minimizations), to derive the optimal ordering of the objects. In fact, constraining the constants $c_{p,k}$ in the model (2) to adhere to one of $N!$ possible spatial ordering would make (2) equivalent to the (NMS) energy, (4). This approach is currently in progress and will be reported in another publication.

However, in this work we use a segmentation based approach to first solve for the regions A_k, and the constants $c_{p,k}$ in the intersection-regions $P_{p,k}$. Then, a comparison of the constants $c_{p,k}, p > 1$ with the object intensities $\{c_i\}_{i=1}^{N}$ would directly give us the ordering of the objects. The main expense in (NMS) and our model (2), is minimizing with respect to the regions A_k. Thus, our algorithm seems to be computationally feasible, since unlike (NMS) which has $N!$ shape minimizations involving $A_k, k = 1, 2, ..N$, we have just one minimization problem to deal with.

4 Level Set Formulation

In this section, a level set implementation of energy (2) is presented. The regions A_k are represented as the interior of level set functions ϕ_k, i.e. $H(\phi_k) = \chi_{A_k}$, $k = 1, 2, ..., N$, where $H(t)$ is the Heaviside function. Thus, we try to recover ϕ_k from I_0. Let $\Phi = (\phi_1, \phi_2, .., \phi_N)$ and $C = (c_{1,1}, .., c_{1,N}, ..., c_{N,1}, \tilde{c})$. We reformulate the problem (2) as the minimization with respect to Φ and C, of following energy:

$$E[\Phi, C] = \int_{\Omega} (I_0 - \sum_{p=1}^{N} \sum_{k=1}^{\binom{N}{p}} (-1)^{p-1} c_{p,k} S_{p,k} - \tilde{c}\tilde{S})^2 dx + \lambda \int_{\Omega} \sum_{k=1}^{N} |\nabla H(\phi_k)| + \beta \int_{\Omega} \sum_{k=1}^{N} \hat{S}(\phi_k) dx \tag{5}$$

where, $S_{p,k}$ is k^{th} unordered product of p functions from $H(\phi_1), H(\phi_2), ..., H(\phi_N)$ and $\tilde{S} = \prod_{k=1}^{N}(1 - H(\phi_k))$. The second term regularizes Φ, and the last term constrains the shape of the 0-levelset of ϕ_k. λ and β balance the three terms.

For simplicity, we will illustrate the $N = 2$ case. The above energy reduces to: $E[\phi_1, \phi_2, c_1, c_2, c_{2,1}, \tilde{c}] =$

$$\int_{\Omega}(I_0 - (c_1 H(\phi_1) + c_2 H(\phi_2) - c_{2,1} H(\phi_1)H(\phi_2) + \tilde{c}(1 - H(\phi_1))(1 - H(\phi_2))))^2 dx$$
$$+\lambda(\int_{\Omega}|\nabla H(\phi_1) + \int_{\Omega}|\nabla H(\phi_2)|) + \beta\int_{\Omega}\hat{S}(\phi_1) + \hat{S}(\phi_2)dx \tag{6}$$

In the above energy (6), it is noted that the first term is equivalent to the multi-phase formulation of [18] for a unique set of constants corresponding to $c_1, c_2, c_{2,1}, \tilde{c}$. However, in our model since occlusions are allowed, segmented objects are represented by $H(\phi_i)$, $i = 1, 2$, whereas, in the multi-phase version of the CV model, objects (i.e phases) are assumed to be disjoint, and hence $H(\phi_1)(1-H(\phi_2))$, $H(\phi_2)(1-H(\phi_1))$, $H(\phi_1)H(\phi_2)$ and $(1-H(\phi_1))(1-H(\phi_2))$ represent the object regions.

The third term is used to impose shape-based constraints such as curvature, and explicit shape on the objects $H(\phi_i)$. This term is used to avoid local minima of the first term in (6) that occur particularly under occlusions. In this work, we only deal with imposing constraints on length and explicit shape. In the (NMS) model, curvature information is used to segment under occlusions.

5 Dis-occlusion

An immediate application of the segmented object-regions A_p and the constants $c_{p,k}$, is finding occlusion relationships between the objects O_p. Suppose that the following assumptions are true:

- Objects do not twist between themselves, i.e. if O_i occludes O_j in some region, O_i is never occluded by O_j in any region.
- The intensity in the regions A_p formed by the objects is close to a constant c_p, and is *different* for objects that occlude each other.

Then the region covering all the objects, $A = \bigcup_{p=1}^{N} A_p$, can be written down as a disjoint union of $2^N - 1$ regions, where the image intensity is close to a constant in each of those regions. Of these, N regions are the visible parts of the objects O_k, with intensity c_k. The rest of the $2^N - N - 1$ regions is where occlusions can possibly occur. The intensities in these regions are close to one of the object intensities, c_k, i.e. the intensity of the object on top. Hence, in one such nonempty occlusion region (WLOG), say $P = \{\cap_{s=1}^{p} A_s\} \bigcap \{\cap_{s=p+1}^{N} \bar{A}_s\}, p > 1$, we can infer that the topmost object is O_t,

$$t = \min_{1 \le s \le p} D(\mu_P, c_s),$$

where μ_U is the average image intensity in a region $U \subseteq \Omega$. In this work, due to the constant intensity assumption in the regions A_p, we use mean-intensity to test for occlusions, and $D(x, y) = |x - y|^2$. This can be easily extended to other measures to handle general image distributions. Also, μ_P can be expressed in terms of the constants $c_{q,k}, q \leq p$, given in (2). We will demonstrate this for $N = 2$ case. From the occlusion model (1), we have:

$$I = c_1\chi_{A_1} + c_2\chi_{A_2} - c_{2,1}\chi_{A_1\cap A_2}$$
$$= c_1\chi_{A_1-A_2} + c_2\chi_{A_2-A_1} + (c_1 + c_2 - c_{2,1})\chi_{A_1\cap A_2}.$$

Thus, if $P = A_1 \cap A_2 \neq \{\phi\}$, then, $\mu_P = \frac{\int_P I dx}{\int_P dx} = c_1 + c_2 - c_{2,1}$. To test for the occlusion relationship between A_1 and A_2, we notice that if

$$(c_2 - c_{2,1})^2 = (\mu_P - c_1)^2 < (\mu_P - c_2)^2 = (c_1 - c_{2,1})^2,$$

then A_1 occludes A_2 and vice versa. Finding occlusion relationships between two objects O_i and O_j gives us relative depth information between them (e.g.O_i is closer than O_j). Secondly, assume that:

- if O_i is closer than O_j and O_j is closer than O_k, implies that O_i is closer than O_k.
- each pair of objects can be compared (either directly or through the above *transitivity* assumption)

Then, we get an ordering of the objects in space, thus solving the segmentation from depth problem for the image.

6 Selective Shape Term

In this work, since we are dealing with occlusions in multi-object segmentation, we use prior shape information of the objects to fill in missing boundaries in occluded regions. However, just adding a shape term as in (6) means that the shape term might influence boundary shapes even in unoccluded regions, where the boundary is unambiguous. Hence, we introduce our shape term in a selective manner. That is, the shape term is allowed to take effect only for occluded boundaries. From the previous section, we see that the constants $c_{p,k}$ encode occlusion information. Hence for a nonempty occlusion region $P = \{\cap_{s=1}^{p} A_s\} \bigcap \{\cap_{s=p+1}^{N} \bar{A}_s\}, p > 1$, we look at the shape term,

$$\sum_{s=1}^{p} \int_{P_s} (\mu_P - c_s)^2 \hat{S}(A_s). \tag{7}$$

Here, $P_s = \bigcap_{\substack{t=1 \\ t\neq s}}^{p} A_t$. We see that the above shape term localizes use of shape only to occluded regions. Firstly, the shape term (7) is defined only on P_s, the region that occludes the object A_s. Secondly, the terms $\hat{S}(A_s)$, that constrain the shape of A_s, are weighted by $(\mu_P - c_s)^2$, which is comparably larger for occluded

regions and minimal for the region on top. We demonstrate this idea for $N = 2$. Denote $I = c_1 H(\phi_1) + c_2 H(\phi_2) - c_{2,1} H(\phi_1) H(\phi_2) + \tilde{c}(1 - H(\phi_1))(1 - H(\phi_2))$. The energy (6) becomes:

$$E[\phi_1, \phi_2, c_1, c_2, c_{2,1}, \tilde{c}] =$$

$$\int_\Omega (I_0 - I)^2 dx + \lambda \Big(\int_\Omega |\nabla H(\phi_1) + \int_\Omega |\nabla H(\phi_2)| \Big) + \beta \int_\Omega \hat{S}(\phi_1) + \hat{S}(\phi_2) dx$$
$$+ \tilde{\beta} \int_\Omega H(\phi_2)(c_{2,1} - c_2)^2 \hat{S}(\phi_1) + H(\phi_1)(c_{2,1} - c_1)^2 \hat{S}(\phi_2) dx \quad (8)$$

Here, the fourth term is the shape term used to nominally influence the shape of the segmented objects to avoid local minima, and the last term weighs the shape term in the regions that occlude A_1 and A_2, i.e. $H(\phi_2)$ and $H(\phi_1)$ respectively. β and $\tilde{\beta}$ balance the shape terms with $\tilde{\beta} \gg \beta$.

7 Numerical Implementation

In this paper, given the binary image S of a prior shape, we use the symmetric area measure to compare shapes. Hence, in (5), the shape term is $\hat{S}(\phi_k) = (H(\phi_k) - S \circ T_k)^2$. T_k are rigid transformations, which also needs to be determined during minimization. To minimize (5), we use a finite difference scheme to solve the resulting Euler Lagrange equations. We present the numerical implementation for $N = 2$ case, shown in (8). Denote $T = [T_1, T_2]$, where $T_k = [\mu_k, \theta_k, \mathbf{t}_k]$, $i = 1, 2$ are rigid transformations with scale μ_k, rotation θ_k and translation $\mathbf{t}_k$. Rewriting (8) using the shape term above,

$$E[\Phi, C, T] =$$

$$\int_\Omega (I - I_0)^2 dx + \lambda \Big(\int_\Omega |\nabla H(\phi_1) + \int_\Omega |\nabla H(\phi_2)| \Big) + \int_\Omega \{\beta + \tilde{\beta} H(\phi_2)(c_{2,1} - c_2)^2)\}$$
$$(H(\phi_1) - S \circ T_1)^2 dx + \int_\Omega \{\beta + \tilde{\beta} H(\phi_1)(c_{2,1} - c_1)^2\}(H(\phi_2) - S \circ T_2)^2 dx \quad (9)$$

Given (Φ, T), the minimizing constants C of the above energy are easily computed as the solution of a linear system. For an index $k \in \{1, 2\}$, let $\bar{k}$ denote its complement. For $k = 1, 2$, the Euler Lagrange equations for (9) are:

$$\delta(\phi_k)\{(I - I_0)(c_{\bar{k}} - c_{2,1} H(\phi_{\bar{k}}) - \tilde{c}(1 - H(\phi_{\bar{k}}))) - \lambda \nabla \cdot \frac{\nabla \phi_k}{|\nabla \phi_k|} +$$
$$\{\beta + \tilde{\beta} H(\phi_{\bar{k}})(c_{2,1} - c_{\bar{k}})^2)\}(H(\phi_k) - S \circ T_k) + \tilde{\beta}(c_{2,1} - c_k)^2 (H(\phi_{\bar{k}}) - S \circ T_{\bar{k}})^2\} = 0$$

$$\frac{\partial \phi_k}{\partial \boldsymbol{n}} = 0 \quad \text{on} \quad \partial\Omega. \quad (10)$$

$$\mu_k \int_\Omega \{\beta + \tilde{\beta} H(\phi_{\bar{k}})(c_{2,1} - c_{\bar{k}})^2)\}(S \circ T_k - H(\phi_k)) \nabla S_{T_k x} \cdot R'_{\theta_k} x \; dx = 0, \quad (11)$$

$$\int_{\Omega} \{\beta + \tilde{\beta} H(\phi_{\bar{k}})(c_{2,1} - c_{\bar{k}})^2)\}(S \circ T_k - H(\phi_k))\nabla S_{T_k x} \cdot R_{\theta_k} x \; dx = 0, \tag{12}$$

$$\int_{\Omega} \{\beta + \tilde{\beta} H(\phi_{\bar{k}})(c_{2,1} - c_{\bar{k}})^2)\}(S \circ T_k - H(\phi_k))\nabla S_{T_k x} \; dx = 0 \tag{13}$$

Given initial values for Φ, C, and T, we use gradient descent to minimize (9), using the above equations.

8 Experimental Results

We present results on synthetic images and a EM (electron microscope) image of erythrocytes, with multiple occluded objects. We demonstrate use of prior shape information (length (Fig.1) and explicit shape (Fig.3,Fig.2) to handle occlusions. Once the mean intensities are obtained for occlusion regions, we show in examples (Fig.3) how occlusion relationships can be deduced for the objects. Finally in (Fig.5 and Fig.6), we see how these relationships have been used to impose shape constraints selectively.

8.1 Segmentation with Length and Explicit Shape

In the images in Fig.1, we assume that only linear segments of objects are occluded. Setting $\beta = 0$ in (6), we see that the length term can be used to resolve segmentation in occluded regions. Starting with initial level sets $\{\phi_k\}_{k=1}^{N}$(N$\leq$ max. number of objects expected) shown in (I), we minimize (6) to obtain segmentation results in (II). The initial level sets have to be overlayed at least

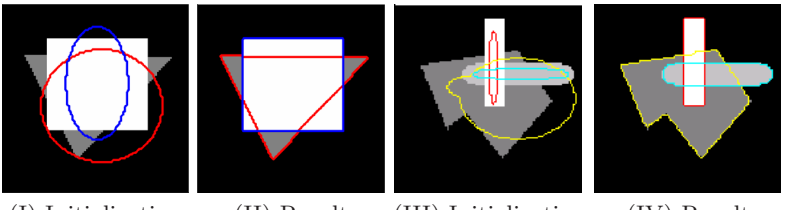

(I) Initialization (II) Result (III) Initialization (IV) Result

Fig. 1. Segmentation of occluded objects with length term

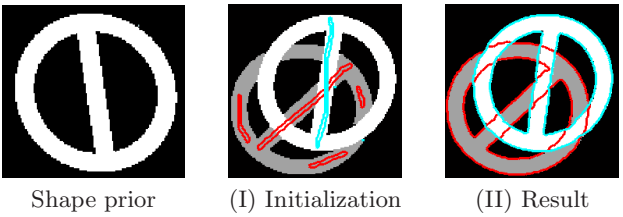

Shape prior (I) Initialization (II) Result

Fig. 2. Occluded boundaries are detected due to the use of shape

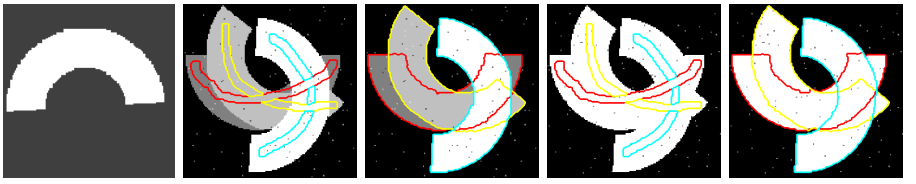

Fig. 3. Segmentation of occluded objects with explicit shape

partially on the corresponding objects, to avoid local minima. The mean intensities can be arbitrarily initialized.

In the next set of examples in Fig.2 and Fig.3, we assume that prior shape information on the objects to be segmented is available. In Fig.2, given an image with occlusions (I), in which the objects can be described by a prior shape (binary image shown on top), we minimize (8) using (10-12) to get the result in (II). The only initial values required here are the initial level sets (shown in I). Using this, a few iterations of the equations (11-12), are used to get an initial guess for the rigid transformation T_k. Fig.3 shows an example for the 3 objects case. Notice that use of prior shape information has resulted in a good segmentation in spite of lack of any intensity information (e.g. Image II).

In Fig.4 (I), we see a given EM image of erythrocytes (red blood cells), which are generally known to have a circular surface structure. Naturally, we use a prior shape of a circle in this case, to resolve occlusions. Starting with a initial guess for the active contours in (II), we arrive at result (IV), which is not possible without prior shape information (III).

8.2 Dis-occlusion

An immediate application of computing the constants $c_{p,k}$ by minimizing (5), is to deduce occlusion relationships between the objects. We demonstrate this procedure for the image shown in Fig.3(I) , with 3 objects. The object regions defined by the characteristic functions $\mathrm{H}(\phi_\mathrm{k}) := \mathrm{H_k}$, with intensities c_k, define 4 occlusion regions, $\mathrm{P}_1 = \mathrm{H}_1\mathrm{H}_2\bar{\mathrm{H}}_3, \mathrm{P}_2 = \mathrm{H}_1\bar{\mathrm{H}}_2\mathrm{H}_3, \mathrm{P}_3 = \bar{\mathrm{H}}_1\mathrm{H}_2\mathrm{H}_3, \mathrm{P}_4 = \mathrm{H}_1\mathrm{H}_2\mathrm{H}_3$. The computed constants $c_{p,k}$ were $c_1 = 128.9, c_2 = 191.9, c_3 = 254.3, c_{2,1} = 129, c_{2,2} = 129.1, c_{2,3} = 192, c_{3,1} = 129.1$. The following table shows a comparison for these intensities in different occlusion regions. The third column shows the mean intensities μ_k corresponding to the regions P_k, that can be computed(shown in the second column) from the constants $c_{p,k}$.

When we compare the mean intensities $\mu_{p,k}$ with c_k, we see that,

$$|\mu_1 - c_2| < |\mu_1 - c_1| \text{ gives, } O_2 \text{ top of } O_1$$

$$|\mu_3 - c_3| < |\mu_3 - c_2| \text{ gives, } O_3 \text{ top of } O_2$$

which gives the ordering(with increasing depth) of the objects as O_3, O_2, O_1.

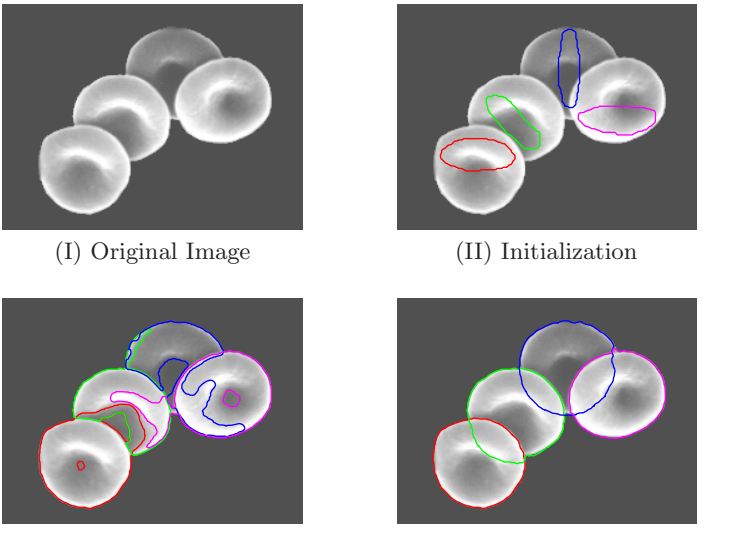

(I) Original Image (II) Initialization

(III) Without shape prior (IV) With a circular shape prior

Fig. 4. Segmentation of erythrocytes in EM image

Table 1. Comparison of mean intensities in different regions

Occlusion Region	Mean,(μ_k)	Values
P_1	$c_1 + c_2 - c_{2,1}$	191.8
P_2	$c_1 - c_{2,2} + c_3$	254.1
P_3	$-c_{2,3} + c_2 + c_3$	254.1
P_4	$c_{3,1} + c_{2,1} + c_{2,2} + c_{2,3} - c_1 - c_2 - c_3$	254

8.3 Selective Use of Shape

Finally, we will see examples where we have used occlusion relationships to impose shape constraints selectively. In Fig.5, we see an image of two objects say (A and B), with A occluding B. In addition, the object on top (A) has sharp features in the intersection region, which we want the segmentation to preserve. Assuming occluded boundaries to be linear, we use the length term to resolve occlusions. In (II), we minimized (6) with $\beta = 0$. The resulting segmentation has correctly filled in the missing linear boundaries for B, but has not segmented A correctly, since the use of length term evenly for both the objects has resulted in the loss of sharp features in A. When we use a selective length term as in (8) with $\hat{S}(\phi_k) = |\nabla H(\phi_k)|$ and setting the parameters $\tilde{\beta} = 0, \lambda \ll \beta$, the required boundaries are computed as needed (III). Notice that the length term is effected only for the object that is occluded (i.e. B), hence preserving the features of A.

A similar example is presented in Fig.6, with use of explicit shape. Here (I) shows two *square* shaped objects A & B with A occluding B, and each with one

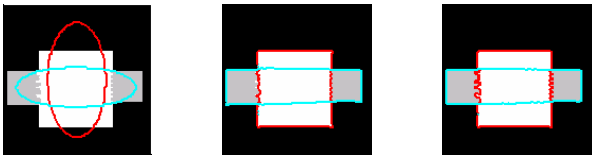

Fig. 5. Selective use of length only for occluded boundaries (I) Initialization (II) Without selective length (III) Selective length term

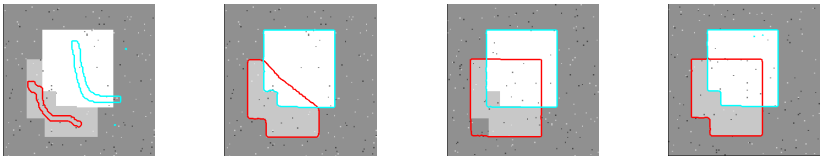

Fig. 6. Selective use of Shape (I) Initialization (II) Without shape (III) Without selective shape (IV) Selective shape

of their corners chipped off. We want our segmentation to be able to complete the missing boundary for B in the occlusion region, and also be able to preserve edges that are not occluded. (II) shows the result when a shape term is not used. (III) shows the result with a uniform shape term as in (8). Notice that the corners of both A & B are not segmented properly, due to the influence of the shape term, even in non-occluded regions. Finally, we get the correct segmentation in (IV), using a selective shape term as in (9). Firstly, use of the shape term has filled the missing boundary of B that has been occluded. Secondly, the shape term is applied only to the occluded object B. Hence the corner of A is recovered. Thirdly, the shape term applied to B is effected only within the object A, thus localizing the effect of shape on B. Hence the corner of B is also recovered.

References

1. V. Caselles, R. Kimmel, and G. Sapiro. Geodesic active contours. In *ICCV*, pages 694–699, 1995.
2. T. Chan and W. Zhu. Level set based shape prior segmentation. In *Proc. CVPR'05*, pages 20–26, 2005.
3. T.F. Chan and L.A Vese. Active contours without edges. *IEEE Trans. Image Processing*, 10(2):266–277, 2001.
4. Yunmei Chen, Hemant Tagare, et al. Using prior shapes in geometric active contours in a variational framework. *IJCV*, 50(3):315–328, 2002.
5. Timothy Cootes, Christopher Taylor, David Cooper, and Jim Graham. Active shape models-their training and application. *CVIU*, 61(1):38–59, 1995.
6. D. Cremers, N. Sochen, and C. Schnörr. Towards recognition-based variational segmentation using shape priors and dynamic labeling. In *Proceedings of International Conference on Scale Space Theories in Computer Vision*, 2003.

7. S. Esedoglu and R. March. Segmentation with depth but without detecting junctions. *J. Mathematical Imaging and Vision*, 18(1):7–15, 2003.
8. S. Kichenassamy, A. Kumar, P. Olver, A. Tannenbaum, and A. Yezzi. Gradient flows and geometric active contour models. In *ICCV*, pages 810–815, 1995.
9. M. Leventon, W. L. Grimson, and O. Faugeras. Statistical shape influence in geodesic active contours. In *CVPR*, volume 1, pages 316–323, 2000.
10. R. Malladi, J.A. Sethian, and B.C. Vemuri. Shape modeling with front propagation: A level set approach. *IEEE Trans. on PAMI*, 17:158–175, 1995.
11. Rousson Mikaël, Paragios Nikos, and Deriche Rachid. Active shape models from a level set perspective. Technical Report 4984, INRIA, October 2003.
12. D. Mumford and J. Shah. Optimal approximations by piecewise smooth functions and associated variational problems. *Comm. on Pure and App. Math.*, 42:577–684, 1989.
13. M. Nitzberg and D. Mumford. The 2.1-d sketch. In *ICCV*, 1990.
14. M. Nitzberg, D. Mumford, and T. Shiota. Filtering, segmentation and depth. *Lecture Notes in Computer Science*, 662, 1993.
15. S. Osher and J. Sethian. Fronts propagating with curvature dependent speed: algorithms based on the Hamilton–Jacobi formulation. *J. of Comp. Phy.*, 79:12–49, 1988.
16. N. Paragios and R. Deriche. Geodesic active regions and level set methods for supervised texture segmentation. *IJCV*, 46(3):223–247, 2002.
17. A. Tsai, A. Yezzi, et al. Model-based curve evolution technique for image segmentation. In *In Proc. CVPR'01*, volume 1, pages 463–468, December 2001.
18. L. Vese and T. Chan. Multiphase level set framework for image segmentation using the mumford and shah model. *IJCV*, 50(3):271–293, 2002.